A review of liquid droplet impacting onto solid spherical particles: A physical pathway to encapsulation mechanisms

Danial Khojasteh[1], Nooshin Moradi Kazerooni[2], Marco Marengo[3,*]

[1] *Water Research Laboratory, School of Civil and Environmental Engineering, UNSW Sydney, NSW, Australia*

[2] *School of Chemical and Petroleum Engineering, Shiraz University, Shiraz, 71348-51154, Iran*

[3] *School of Computing, Engineering and Mathematics, University of Brighton, BN2 4GJ Brighton, United Kingdom*

Abstract

Encapsulation has received a surge of interest in the biotechnological, chemical and pharmaceutical fields and other industrial processes, owing to numerous applications such as in fluidized catalytic cracking, antenna and wire fabrication, catalytic reactions, and process industries. For example, encapsulation is a technique used to entrap active agents within a carrier material and can be achieved through impact of droplets of encapsulating material on the solid particles of active agents. Considering the importance of dynamics of drop-particle collision, which directly affects the quality of film deposition during encapsulation, the current review is presented to investigate various aspects of drop impact on dry solid spherical surfaces, which is still lacking in the existing literature and aims at encouraging more researchers to study this topic. Also, this review covers frequent examples of droplet impingement onto curved surfaces, with a focus on the latest scientific findings in droplet impacting solid spherical surfaces.

Keywords: Encapsulation, Droplet impact, Spherical surface, Wettability, Multiphase Flow.

Nomenclature

CA	Contact angle
Ca	Capillary number
D	Droplet diameter
D_0	Droplet's initial diameter
D_{max}	Droplet's maximum spreading diameter
D*	Ratio of particle's diameter to drop's diameter
FCC	Fluidized catalytic cracking
H	Hydrophobic
HP	Hydrophilic
ND	Not defined
MED	Multi-effect desalination
Oh	Ohnesorge number ($oh = \sqrt{We}/Re$)
Re	Reynolds number ($Re = \rho_f v D / \mu$)
SH	Superhydrophobic
v	Impact velocity
We	Weber number ($We = \rho_f v^2 D / \sigma$)
β	Retraction coefficient
ρ_f	Fluid density
σ	Surface tension
θ	Equilibrium contact angle
μ	Dynamic viscosity

1. Introduction

The phenomenon of liquid droplets undergoing collisions with solid spherical objects and fibres is ubiquitous in nature, daily life and in a wide range of industrial applications [1-4]. One of these applications is, for example, the analysis of rain drops impinging cables, wires and antennas, important in describing icing processes. Ice formation caused by impinging droplets can be prevented by minimising the contact time to promote rapid shedding of droplets before ice can nucleate on the surface. Also, by a combination of surface roughness, chemistry and topographical modifications, ice nucleation by drop impaction can be delayed [5,6]. In process industries, the interaction of liquid droplets with a solid surface is of paramount importance in many multiphase flow systems, such as heterogeneous catalytic reactions. In trickled-bed reactors, enough wetting of catalyst particles is essential for high catalyst efficiency and process performance. In fluidized catalytic cracking (FCC), where the feed is introduced through atomizers and the sprayed droplets vaporize by contacting the hot solid catalyst, adequate contact of liquid droplets with the solid surface of catalysts is required to ensure a fast vaporization and to facilitate the cracking reactions. In such reactors, the droplet size has a major effect on the heat transfer between droplet and catalyst particles. An optimized droplet size provides high rates of heat transfer and hence high conversion [7, 8]. In the film-boiling regime, hydrocarbon vapour produced from evaporation creates a thin vapour layer, and thus, a non-wetting condition arises during collision [9]. This phenomenon leads to decreased heat transfer during drop impact since the vapor layer acts as a thermally insulating film. One of the important parameters characterizing such processes is the heat flux density at various thermodynamic regimes and the substrate structures. Hence, understanding the heat transfer during drop impact in the film boiling regime is of essential significance [10]. In multi-effect desalination (MED) evaporators, seawater is sprayed on a tube bundle which carries hot steam, in order to achieve distilled water inside the tubes [11]. Multilayer drop deposition, with several uses in sensors, polymer electronic

devices, integrated optics, biocompatible scaffolds and drug delivery systems, can be readily obtained and tailored on the substrates of different shapes. In these processes, the average contact time of a droplet and its target is the key factor which significantly affects the bilayer thickness [12]. Liquid droplet impingement on a spherical surface has a great impact on the rapidly growing field of droplet-base microfluidics, where numerous techniques are being developed to control, manipulate, and functionalize droplets [13-15]. Several applications of droplet impacting onto spherical surfaces are depicted in Fig. 1. Droplet-based microfluidics holds a great promise in a broad range of areas, e.g. single cell analysis, cell-based assays, and drug discovery, most of them requiring biological materials (cells, organisms, proteins, beads) to be encapsulated inside liquid droplets [19, 20]. The encapsulation technology, which has attracted a flow of interests, offers a tremendous tool for many industrial applications especially in the biotechnological, chemical and pharmaceutical areas. One of the highlights of encapsulation is that each drop can be regarded as a compartment within which individual reactions can be carried out in a physically and chemically isolated system [21, 22]. This compartmentalization, which successfully mimics the effect of the cell boundary, offers key advantages, such as flexible control of extracellular environments and prevention of active evaporation and degradation, as well as cross contamination [23, 24].

One of the most widely applied encapsulation techniques is the so-called spray drying, owing to the fact that it provides good flexibility and a continuous, economical operation. The spray drying is a conventional method of converting feedstock from a fluid state to dried particles by spraying the coating agent onto the particles. After drop-particle collision, the sprayed droplets spread on the surface of the particles. The coated particles are exposed to a flow of heated air leading to very fast liquid evaporation. This is the preferred technique for drying thermally-sensitive materials such as pharmaceuticals, food and biochemicals [25, 26].

As listed by Nedovic et al. [27], the majority of encapsulates are spray-dried, and the rest are prepared by:

- Spray-chilling, which is similar to spray drying except that the liquid is sprayed into a chamber where particles are formed from cooling and solidifying the droplets rather than from solvent evaporation.

- Freeze-drying, which is a water removal technique from the frozen state. In this technique, liquid or slurry materials are frozen and the dried through a sublimation process. Sublimation takes place either under vacuum or under atmospheric pressure.

- Melt extrusion, which is an effective processing technology in developing pharmaceuticals, consisting of melting a drug substance and forcing it through a die, under controlled conditions to form a new material.

- Melt injection, in which a solid material is dispersed into liquid hydrocarbons, and then injected thorough an orifice into a bath of cold liquid e.g. liquid nitrogen or isopropanol.

- Emulsification, which is the process by which the dispersed phase is broken up into small droplets, is generally applied for the encapsulation of bio-actives in aqueous solutions, which can either be used directly in the liquid state or can be dried to form powders.

A schematic view of these processes is illustrated in Fig. 2.

In the biological field, droplet factors such as containment and its volume from few femtoliter to hundreds of picolitre, are important for the encapsulation of cells in droplets [22, 34]. Additionally, it is of essential significance to make sure that the integrity of droplets is maintained, i.e. merging or splitting should be avoided, so that cells within droplets remain encapsulated, and are not transferred either to the continuous phase or to the adjacent droplets [34].

In an ideal world, the solid particles to be encapsulated should have high density, high wettability and a spherical shape. This is mainly due to the fact that in this way they provide (i) the minimum momentum transfer of solid particles (for a similar size of drops and particles), (ii) the highest liquid coverage without dry spots and film break-up and (iii) the lowest possible surface area for a given size of particles, whereby

less coating material is then required. Moreover, sharp edges can potentially damage the coating during handling steps [35]. For an efficient encapsulation operation, a successful droplet deposition on the particle is necessary, followed by an adequate spreading and coverage of the encapsulating material on the surface of the particles. Hence, it is of essential importance to prevent splashing or rebound of the droplets and ensure high liquid wettability and adhesion [25, 36]. In the real world, particles either can have various geometries and surface features, and therefore the liquid may not be able to cover uniformly their surface, or the wettability is low and therefore the coating presents holes and different thicknesses, so only a rather empirical approach to the various parameters and factors is essential to optimise the processes.

Since the geometrical characteristics of the particles can be complex to deal (consider for example the drop impact onto cubic crystals) and it mixes with other parameters like contact angle, size, surface roughness and so on, here we only propose an introduction of the idealised process of liquid drop impacting onto still dry surfaces of spherical forms, in order to make easier the understanding of the physical principles of the interaction between drops and particles leading to encapsulation.

2. Droplet impact onto spherical objects

As mentioned in the previous section, in a broad range of applications, the droplets impact small, curved or spherical surfaces (cables, wires, tubes, catalysts, active agent of encapsulation, etc.). The dynamics of droplet impact onto dry small, curved targets, like spheres and particles, differs from the droplet impact onto large, flat substrates [37-39]. While there is a vast amount of literature considering droplet impact on solid, flat surfaces, very limited experimental and numerical investigations are available on impingement of droplet on solid spheres and particles. The morphology of a droplet after colliding with a curved surface is influenced by the contact angle (CA) [7, 40], the geometry of the surface [41], liquid properties (viscosity, density, surface tension) and kinematic parameters [42, 43]. To examine the aforementioned

6

factors, a relatively small - but growing - body of literature has already been dedicated to this research topic. Depending on droplet and target sizes, and the receding CA, the drop can either bounce off or adhere to the interface. The rebound appears when the receding CA of the surface is greater than 90º and above a critical impact velocity, whereas it occurs after that the droplet oscillates, and finally bounces off the surface. In case of adhesion, when the sum of normal components of the forces acting on the droplet bulk in the outward direction (for example, buoyancy force) is lower than the sum of the normal components in the inward direction (for example, gravity and adhesion forces), the liquid stays in equilibrium on the solid substrate, and an equilibrium CA is reached [44]. When a droplet undergoes a collision with a sphere, a radial flow emerges due to the momentum normal to the surface. The available impact kinetic energy is converted into surface energy and dissipated by viscosity effects. The impacted drop spreads over the surface until it reaches a maximum spreading diameter, and then it may recoil.

For droplet impact phenomenon, if resistive forces (for example, hydrostatic pressure force) are strong enough, the droplet will decelerate after the collision. Then, after reaching a certain distance less than the droplet diameter, the velocity will become zero finally. This impact velocity is defined as droplet critical velocity [44]. For curved surfaces, there is a critical impact velocity beyond which the drop cannot be retained at the gas–liquid boundary. This critical impact velocity is of considerable significance for the processes (e.g., flotation) where a droplet should entrap a spherical object. The critical velocity decreases with a decrease of surface tension and surface hydrophobicity, as well as with an increase of drop size and the ratio of surface-liquid density [44, 45].

In a benchmark study by Dubrovsky et al. [46], for droplet-target size ratio greater than unity, four distinct interaction regimes were identified: capture (the target is completely encapsulated by the droplet fluid), shooting through (satellite droplets are formed), bubble formation (air bubbles entrained into the lamella) and drop destruction (the drop broken into many parts during the collision). When the particle density ρ_s

and/or the impact *Re* is low, the "capture" scenario is more probable, while the other three scenarios are observed with an increase in *Re* and particle inertia.

Droplets may also impinge on a liquid film during different industrial processes in which the pre-existing film is usually produced by the previous impact [47]. Generally, depending on the application aspects, various shapes of the liquid film may be involved which are commonly determined by the substrate that the liquid adheres to, and hence, the film shape can be varied by altering the substrate shape [48]. The outcomes of a single droplet impacting on a curved surface covered by a thin liquid film, which can be considered a wetted surface, is also remarkably different from the case of a flat liquid film [48]. For drop impact on cylindrical and spherical liquid film, it has been reported that the outcomes after impact is greatly influenced by the cylinder-drop and sphere-drop curvature ratio [48, 49]. For the impact on the wetted cylinder with small curvature ratios, rebound occurs at low impact velocities and high viscosities and as the impact velocity increases, spreading phenomenon is observable. By further increasing the impact velocity, the liquid droplet overcomes surface tension to rise and create a liquid sheet, with different characteristics from the crown liquid sheet during drop impingement on a flat film. Finally, splashing occurs at higher velocities. On the other hand, for the wetted cylinder with the larger curvature ratio, rebound, coalescence, dripping and disintegration are observed in succession as the impact velocity increases [48]. Also, for droplet impact on a wetted sphere, spreading at low impact Weber numbers and splashing phenomena at high Weber numbers have been reported [49]. However, droplet impact on wetted particles is not the focus of this review paper.

The next sections aim at providing a panoramic overview of the recent developments in the broad area of dynamics of drop impacting on dry, solid, spherical surfaces with a focus on encapsulation. To serve this purpose, drop-sphere impact and possible collision outcomes are classified based on the surface wettability for hydrophilic (HP), hydrophobic (H) and superhydrophobic (SH) substrates. Moreover, the

8

current literature about impacts of droplet onto spherical heated surfaces is analysed to provide a better understanding also for the diabatic conditions. The experimental and numerical investigations of droplet impacting onto spherical surfaces are summarized in Table 1 and Table 2, respectively. According to these tables, it is feasible to better understand the effects of different factors (i.e. *We*, *Re*, CA, fluid properties, drop diameter to particle diameter ratio, etc) on outcomes of drop-particle collision. Also, Weber ranges for all these experimental and numerical studies are illustrated in Fig. 3. As it can be seen in this figure, experimental investigations cover a wider Weber range compared to numerical ones.

2.1. Impact on hydrophilic spherical particles

The dynamics of liquid droplets impinging a solid sphere was coined by the pioneers Levin and Hobbs [68], when they analysed the splashing behaviour of a drop impacting onto a curved substrate whose radius of curvature is much larger than the drop radius. Later, an experimental investigation was carried out by examining the impact of droplet (impact velocity of 6-13 m/s) on cylindrical wires with diameters of 0.8-1.3 mm [69]. A three-dimensional model of free surface flows was developed with the ability of predicting the dynamics of droplet impacting an HP substrate of arbitrary shape. In this study, it was reported that after impacting on small cylinders, droplets left the surface since there is not enough surface area, i.e. adhesion, for the liquid to remain attached [60]. In another experimental study regarding the normal collisions of water drops against a stainless-steel disk, Rozhkov et al. [50] showed that the drop spread beyond the small disk in a shape of a central cap surrounded by a thin and conical lamella bounded by a thicker rim. Bakshi et al. [37] and Gac and Gradon [62], by looking at the film thickness variation, demonstrated that the drop behaviour comprises three distinct phases including i) initial drop deformation, ii) the inertia dominated phase, and iii) the viscosity dominated phase; The first two phases collapse onto each other for different values of *Re* for a given droplet-target combination (ratios are 1.23 and 2.3).

For the impacts of water and diesel drops on rods when the rod tip is convex, the experimental tests indicated that diesel drop breaks up more readily than water due to its low surface tension [51]. Juarez et al. [52] found that the lamella extension, followed by a subsequent breakup of the outer rim, is controlled by length scales which are dimensionally comparable with the impacting drop diameter. In addition, depending on the number of edges, two distinct splashing regimes were observed and illustrated in Fig. 4; regular splashing (for $3 \leq n < 8$) and irregular splashing (for cylinder and $n \geq 8$), where n is number of edges of a polygon (regular splashing is used whenever the number of filaments is equal to the number of target vertices; irregular splashing is used whenever the number of filaments and their location are independent of the target geometry or number of vertices).

In more recent studies, the collision behaviour of a smaller particle into a larger stationary droplet was investigated both numerically and experimentally by Mitra et al. [44]. Taking into consideration all forces acting on the process, it was found that the effects of pressure and capillary forces were significantly dominant during the interaction process. The effect of different Weber (We) numbers on glass ballot in particle impact on water droplet is illustrated in Fig. 5. Sechenyh and Amirfazli [54] noted that the drop envelops the particle at the first stage, promoting incorporation of a particle inside the fluid volume, even if the glass particles are H. At moderate Re and We, the effect of aspect ratio of the sphere to the drop, D*, on spreading and retraction of droplet hitting a steel, spherical surface was investigated. It was demonstrated that the thickness of the liquid film, h_L, can be well approximated by $h_L \sim h_{L,f} (1+3/4 \, D^{*-3/2})$, where $h_{L,f}$ denotes the film thickness of drop impact on a flat substrate [70]. Recently, a further regime was revealed for droplet collisions with small particles (D* < 3.3) in which a crown is generated around the particle surface and passes around it. This is depicted in Fig. 6, where the film ejection is observed to occur in the same direction as the droplet motion (downward).

2.2. Impact on hydrophobic spherical particles

Analysis of droplet impingement on hydrophobic (H) particles leads to identifying some substantial differences in the behaviour of the liquid drop after the impact. In one of the earliest 2D numerical analysis of an impact on a sphere (with an equilibrium CA of 107º), it was demonstrated that drop spreads over the curved target and becomes thinner as it moves along the curved substrate, while the surface tension dominates the retraction phase until the drop is bounded to the surface [63].

Yan-Peng and Huan-Ran [61] developed an innovative numerical model by coupling the level-set method and the interfacial cell immersed boundary layer. They found that a local breaking phenomenon (creating a bowl shape) may occur in the centre of the droplet when hitting a smaller sphere during the recoiling stage. For a polystyrene particle (H surface) and mid-air collision (both droplet and particle are launched in the air for collision), Sechenyh and Amirfazli [54] observed the generation of an axi-symmetric liquid jet, which eventually breaks into satellite drops. They also reported that for $We > 162$, a conical lamella is formed outward of the particle surface. In addition, the air entrainment facilitates the splash occurrence when the edge of the spreading liquid lifts up from the surface [56]. In another numerical study on droplet-particle collision, it was found that the inertial forces dominate over the viscous, gravitational and surface tension forces at the early stages of impact [65]. Liu et al. [66] carried out a numerical analysis by employing a coupled level set and volume-of fluid (VOF) method, concerning the impact outcomes after drops hit tubular surfaces with different hydrophobicity values (CAs of 107º, 120º, and 135º, respectively). The results showed that, for a given impact velocity, an increase in the hydrophobicity is decreasing the maximum spreading ratio on the curved substrate (Fig. 7 for CA ≥ 135°), Furthermore, the liquid film splashes into several parts, rather than retracting as a single liquid bulk. Also, the key factors defining spreading, splash, and rebound, are pressure and velocity fields inside and outside the liquid film. In other words, it is the pressure difference between the centre of the spreading film and the its edge that forces

the droplet to stretch over the curved surface. To better understand the drop impinging an H surface, Fig. 8 depicts droplet collision onto a glass sphere with CA of 118º, and for different impact velocities. Mitra et al. [57] carried out a further experiment to analyse the collision interactions between a droplet and an H particle for $0.9 < We < 47$. At low We, periodic spreading and recoiling phenomena were observed, characterized by the dynamic CAs (dynamic CA is defined when the three-phase boundary is moving, and is referred as advancing and receding angles). For $We > 20$, a transition occurs from deposition to complete wetting, as a thick rim grows at the edge of a thin lamella. Khojasteh et al. [11] indicated that an increase of the equilibrium CA of an H substrate leads to a lower D^* due to the fact that the droplet needs a higher energy to cover a surface.

Considering soft surfaces, in an experimental study of the impact of water drop on convex, hemispherical polydimethylsiloxane (PDMS) surfaces, the effects of the elastic modulus of the solid object, the diameter ratio, and the We on the dynamic CA were examined [58]. It was observed that, at relatively high We ($We = 81$), surface with a higher curvature increases the retraction of the spreading drop, due to the difference of energy dissipation induced by the curvature of the surface. This behaviour can be elucidated in terms of surface deformation upon impact, which absorbs a fragment of the impact kinetic energy. Additionally, a droplet experiences a more pronounced recoiling phenomenon as the curvature of the surface increases. This is demonstrated in Fig. 9, where retraction coefficient (β) can be compared for different particle to drop diameter ratios. This coefficient is defined as $\beta = (\alpha_{max} - \alpha_{max})/ \alpha_{max}$; where α is the spreading angle.

2.3. Impact on superhydrophobic spherical particles

There is a very limited number of experimental and numerical studies concerning droplet hitting a SH surface. For an impact with a spherical substrate with an equilibrium CA of 160º and $We = 8$, Liu et al. [53] noted that the drop spreads radially at the first phase and then, with the start of drop recoil, this

spreading becomes increasingly anisotropic. An interesting phenomenon during this process is that the retraction of drop begins in straight (width or axial) direction, while it continues to spread in the azimuthal (curved) direction. This is mainly due to the fact that the momentum in the azimuthal direction is always greater than that of the axial direction. This is because the momentum in the axial direction starts to reverse its direction, while the azimuthal momentum stays positive and increases slightly. In a later paper, Liu et al. [66] observed, using a CFD analysis by coupling VOF and level set methods, the drop impact in both radial and axial directions for an impact velocity of 1.2 *m/s* on a curved target with CA of 153º (D* = 2.3). When the spreading ends at its maximum spread, the droplet bounces off the substrate directly, without recoil, and then it divides into three distinct parts, rebounding to even a higher height than previous stage (rebound of the full-spread droplet). Figure 10 summarises the outcomes of droplet-particle collision for a SH surface and for different *We* and D* ratios [71].

Khojasteh et al. [11] explored the effects of *We*, equilibrium CA and surface curvature on impact dynamics. The obtained maximum spreading diameters were compared to those obtained from previous empirical and analytical correlations. It was found that these pre-established models are not capable of predicting the maximum spreading diameter for impact on spherical particles since the spreading diameter is considerably higher when hitting a sphere than hitting a flat one. This is mainly due to the effects of centrifugal force rather than gravity force. A modification of the mentioned available correlations for predicting maximum spreading diameter was proposed by the authors, so that they could be used for droplet impact on spheres, as presented in Table 3. According to this table, the modified model of Akao et al. [72] is the most accurate one to predict the drop maximum spreading diameter after impacting a curved target. These correlations are valid for low-viscosity fluids impacting on H and SH spherical surfaces and for *We* up to 30. Figure 11 depicts the time evolution of the ratio of drop diameter and its initial diameter prior to impact, for various impact conditions. Based on several numerical simulations, an

accurate model was presented to evaluate the maximum deformation of low viscosity fluids onto H and SH spherical solid surfaces for low *We* (*We* < 30) as [67]:

$$\beta_{max} = 1.54We^{0.3}(3.52-\theta)^{0.25} \tag{1}$$

where β_{max} is the ratio of the maximum spreading diameter of the droplet to its initial diameter, and θ is the equilibrium CA in radians. It was also found that the spreading diameter increases with the impact velocity, an increase of the spherical surface diameter, a lower surface wettability, and a lower surface tension [67].

2.4. Impact onto heated spherical particles

Although the focus of many researches regarding drop impingement has been on adiabatic impact dynamics, most of the applications of this phenomenon involve relatively high temperatures [76]. In processes like spray-cooling, the heat transfer is highly affected by the droplet impact dynamics [77]. Also, in fluidized catalytic cracking, which is utilized in petroleum industry, the conversion of heavier fractions to lighter hydrocarbons takes place by effective contact of feed droplets with catalyst particles at high temperatures. The feedstock is at the bottom of the riser in which the atomized drops hit the hot catalyst particles, so the drops may spread over, splash or bounce off these particles after impinging. However, in order to have a higher yield, it is necessary to establish an appropriate contact of droplets and particles in a way that drops evaporate immediately. For a hot surface, it is observed that droplet spreading pattern is considerably influenced by the heat transfer characteristics at the interface, which is due to complex interaction involving momentum transfer and heat and mass transfer [7]. The complexity associated with the dynamics of impact is due to the inter-dependence of momentum, heat, and mass transfers between the two phases, which depend on impact velocity, size of droplet and target, CA, surface tension, surface characteristics, heat capacity and temperature of the target [64].

In an experimental investigation concerning the impact of subcooled water, isopropyl alcohol and acetone droplets onto a highly thermally conductive spherical target with a surface temperature varying between 20 $^\circ$C and 250 $^\circ$C, wetting and non-wetting contact phases were found. For the film boiling regime, the wetting process was hindered by a thin vapour film at the contact zone, leading to a smaller temperature drop of surface. Besides, when the temperature of the target surface is much higher than the saturation temperature of the drop, a vapour film emerges at the interface, acting as an insulating layer that diminishes the heat transfer. Therefore, occurrence of nucleation and hence boiling is prevented, and droplet evaporates gradually [7]. Figure 12 represents the droplet deformation after hitting an HP surface with temperature of 250 $^\circ$C. As it is deduced from the figure, the droplet continued to elongate axially during the recoiling phase, until it gets detached from the target. Moreover, vapour is generated at the interface due to considerable temperature difference of surface and droplet. Due to presence of this vapour film, the surface of the target becomes a SH surface with a CA of about 180°. In a numerical study regarding water droplets of various diameters impacting a hot solid particle with surface temperature of 250 $^\circ$C, it was found that drop spreading depends on several factors including surface tension, viscous forces and *We*, while droplet recoiling is highly dependent on *Re* number since the fluid advection increases the rate of heat transfer. Finally, the drop rate of evaporation strongly depends on the capillary length of the fluid and the stability of the vapour film that forms beneath the drop [64]. In a recent study, the droplet-particle (HP brass) interaction for size ratio less than one, for 8 < *We* < 195 and particle surface temperature range of 250-350 $^\circ$C was examined. According to the obtained results, two distinct regimes are found for non-wetting behaviour of droplet: rebound and complete disintegration. The experimental measurement of the dynamic CA indicates that, for low *We* (range stated above), it lies in a range from 120° to 160°, demonstrating the high hydrophobicity of the particle surface in film boiling regime [78]. In another experimental study, for 1 < *We* < 47, Mitra et al. [57] studied the collision of a droplet with a

stationary thermally conductive H particle in low *We* (in range of 1-47) and for drop diameter to brass particle diameter ratio of about 0.85. During the rebound phase, no tangible temperature reduction was observed due to the non-wetting behaviour of droplet. With an increase in *We*, a significant decrease in particle temperature is reported in the range of $\Delta T = 10\text{-}70 \, ^\circ C$. This is why the higher wetted area and nucleate boiling of the secondary droplets observed in disintegration outcome are attributed to this temperature reduction. The head-to-head impingement of diesel fuel droplets onto an HP spherical target (made of polished brass) was studied experimentally for the surface temperatures from 140 to 340 $^\circ C$. It was found that a higher surface temperature and *We* result in droplet disintegration. Furthermore, with an increase in particle temperature, the droplet vibrates on the particle surface, causing an oscillatory motion after reaching the maximum spreading diameter. This is explainable by an alteration in fluid physical properties, in particular viscosity, due to heat transfer at the solid-liquid interface [59].

3. Conclusions

The dynamics of droplet impact on particles is a key feature in a wide range of natural and industrial processes, e.g. surface roughness modification, fluidized catalytic cracking, trickled bed reactors, multi-effect desalination evaporators, multilayer film deposition, bloodstain pattern analysis and rain drops impinging cables, wires and antennas, among which encapsulation has received considerable attention in the biotechnological, chemical, pharmaceutical and food industries. Encapsulation offers an effective tool to cover an active compound with a protective wall material and as a result, delivers a multitude of advantages including protection of actives against evaporation and undesired chemical reactions, controlled delivery and preservation of stability. Due to the fact that the collision of the coating droplets with the particles of active agent, and adequate spreading of the coating on the particle is one of the most important steps of encapsulation, final product properties is significantly affected by the parameters of

impact. In this regard and considering the fact that in almost all of the mentioned applications, the particle on which the droplet impacts is spherical or almost spherical, a comprehensive review is essential to elucidate the underlying physics of the drop impact upon solid curved and spherical surfaces. Hence, this paper covers the head-to-head impact of droplet-particle, and the possible collision outcomes are classified based on the surface wettability. These outcomes are qualitatively presented in Fig. 13 for hydrophilic, hydrophobic and superhydrophobic surfaces as a function of We and D*. Further, to better summarise the effect of We, for $0.1 < We < 1000$; droplet gently lands on and covers HP surface. The collision outcome almost remains same for this range of We is due to high wettability of the target surface. As the droplet goes down over the particle, a layer of liquid sticks to the particle surface which preserves the droplet from breaking up or forming a lamella [56]. Further, by increasing We, the time to reach the maximum spreading diameter decreases. The trend of normalized diameter for impact on H and SH surfaces are similar. For these two surfaces and for low We, the drop spreads over the surface and reach its maximum diameter and then retracts and is usually followed by a partial or complete rebound [11]. For higher We, liquid films in each side of the particle are formed [56].

Several conclusions may be drawn from this review as follows:

(1) The most typical outcomes of the drop impacting spherical surfaces include (a) spreading, (b) complete rebound, (c) splash, and (d) a final deposition stage after several spreading and recoiling processes.

(2) For droplet impact on hydrophilic spherical particles, it was reported that there are three distinct phases regarding droplet behaviour including initial drop deformation, the inertia dominated phase, and the viscosity dominated phase. During the interaction process, the effects of pressure and capillary forces were significantly dominant over other forces. For the moderate ranges of Re and We, the north pole of the sphere experiences a higher pressure while a thin layer of liquid film forms there and a rim occurs near

the front of this liquid film. Recently, a new outcome of droplet and small particle impact was found in which a non-breaking droplet forms a stable crown along the particle surface.

(3) Regarding droplet impingement on hydrophobic particles, the splash phenomenon is accelerated since an air entrainment is formed which lifts up the edge of the spreading liquid from the surface. For low impact *We*, the periodic spreading and recoiling phenomena are readily observable, characterizing by the dynamic contact angle. Moreover, an increase in contact angle of a hydrophobic target results in a lower normalized diameter after impacting a spherical surface which is due to the fact that the droplet needs little energy to cover a surface with lower contact angles.

(4) Only few numbers of experimental and numerical researches are available in the literature that examine the collision of a droplet with solid superhydrophobic spherical substrates. As the spreading diameter is significantly higher when hitting a spherical particle, the available pre-established correlations are incapable of predicting this diameter. However, a practical relation is recently presented to carefully predict the maximum spreading diameter for impact of low viscosity fluid in low *We* (see Equation (1)). It was also revealed from the analysis of the gravity and centrifugal forces that it is the latter one that causes a higher spreading ratio on curved superhydrophobic surfaces.

(5) With respect to drop impact onto heated spherical particles, it was noted that for the film boiling regime, the wetting process is prevented by a thin vapour film at the contact zone, leading to a smaller temperature drop of surface. Due to presence of this vapour film, the surface of the particle becomes a superhydrophobic surface. Additionally, the drop spreading on heated spheres is related to several factors such as surface tension, viscous forces and *We*, while droplet recoiling is strongly dependent on *Re* number. For impact of diesel fuel droplets onto hydrophilic spherical particles, the maximum spreading diameter increases with a rise in impact *We* and a decrease in particle temperature.

4. Future Outlook

I.   Determining and elucidating the underlying mechanism of splashing threshold is of practical significance and importance. It is recommended more studies should be dedicated to this topic to characterize the resulting splash for spherical surfaces. Size, number, and trajectories of generated droplets (after splash) are important (e.g., size in aerosol generation and trajectory for uniform coating) [38].

II.   In industrial and practical applications, most of drop-particle collisions are oblique to the surface. In this case, the flow pattern is not symmetrical, and the fluid possibly flows downward after the impact. This topic deserves to receive more attention by the scholars.

III. While superhydrophobic surfaces have attracted a great deal of attention among researchers and industrialists, the impact of droplet on these particles are not fully understood. To illustrate, these surfaces are employed to reduce the contact time of impacting drops and substrates which is vital in managing heat and mass transfer. However, the dependence of the contact time on impact velocity and the scales of surface structure remains uncertain and requires further attention [71].

5. References

[1] Grishaev, V., Iorio, C.S., Dubois, F. and Amirfazli, A., Impact of particle-laden drops: splashing criterion, Atomization and Sprays, vol. 27, no. 5, 2017.

[2] Kamali, R., Khojasteh, D., and Mousavi, S.M., Newtonian and non-Newtonian Droplet Impact onto a Heated Hydrophobic Solid Surface, 24th Annual International Conference on Mechanical Engineering-ISME, Yazd, Iran, April 26-28, 2016.

[3] Khojasteh, D., M. K. D. Manshadi, S. M. Mousavi, and R. Kamali. Droplet Impact on Superhydrophobic Surface under the Influence of An Electric Field. Paper presented at the annual meeting

for 3rd Annual International Conference on New Research Achievements in Chemistry & Chemical Engineering, Tehran, Iran, 2016.

[4] Manshadi, M. K. D., D. Khojasteh, A. Mansoorifar, and R. Kamali. Efciency Enhancement of ICEK Micromixer by a Rectangular Obstacle. Paper presented at the annual meeting for 3rd Annual International Conference on New Research Achievements in Chemistry & Chemical Engineering, Tehran, Iran, 2016.

[5] Wang, X., Naterer, G.F. and Bibeau, E., Convective droplet impact and heat transfer from a NACA airfoil. Journal of thermophysics and heat transfer, vol. 21, no. 3, pp.536-542, 2007.

[6] Kreder, M.J., Alvarenga, J., Kim, P. and Aizenberg, J. Design of anti-icing surfaces: smooth, textured or slippery?, Nature Reviews Materials, vol. 1, no. 1, p.15003, 2016.

[7] Mitra, S., Sathe, M.J., Doroodchi, E., Utikar, R., Shah, M.K., Pareek, V., Joshi, J.B. and Evans, G.M., Droplet impact dynamics on a spherical particle, Chemical Engineering Science, vol. 100, pp.105-119, 2013.

[8] Gupta, A. and Rao, D.S. Model for the performance of a fluid catalytic cracking (FCC) riser reactor: effect of feed atomization, Chemical Engineering Science, vol. 56, no. 15, pp.4489-4503, 2001.

[9] Ge, Y. and Fan, L.S., Droplet–particle collision mechanics with film-boiling evaporation, Journal of Fluid Mechanics, vol. 573, pp.311-337, 2007.

[10] Breitenbach, J., Roisman, I.V. and Tropea, C. Heat transfer in the film boiling regime: single drop impact and spray cooling, International Journal of Heat and Mass Transfer, vol. 110, pp.34-42, 2017.

[11] Khojasteh, D., Bordbar, A., Kamali, R. and Marengo, M., Curvature effect on droplet impacting onto hydrophobic and superhydrophobic spheres, International Journal of Computational Fluid Dynamics, vol. 31, pp.310-323, 2017.

[12] Lee, M., Park, W., Chung, C., Lim, J., Kwon, S., Ahn, K.H., Lee, S.J. and Char, K., Multilayer deposition on patterned posts using alternating polyelectrolyte droplets in a microfluidic device, Lab on a Chip, vol. 10, no. 9, pp.1160-1166, 2010.

[13] Manshadi, M.K.D., Khojasteh, D., Mohammadi, M. and Kamali, R., Electroosmotic micropump for lab- on- a- chip biomedical applications, International Journal of Numerical Modelling: Electronic Networks, Devices and Fields, vol. 29, no. 5, pp.845-858, 2016.

[14] Shabankareh, I. Z., Mousavi, S. M., and Kamali, R., Numerical study of non-Newtonian droplets electrocoalescence, Journal of the Brazilian Society of Mechanical Sciences and Engineering, vol. 39, no. 10, pp.4207-4217, 2017.

[15] Taassob, A., Manshadi, M.K.D., Bordbar, A. and Kamali, R., Monodisperse non-Newtonian micro-droplet generation in a co-flow device, Journal of the Brazilian Society of Mechanical Sciences and Engineering, vol. 39, no. 6, pp.2013-2021, 2017.

[16] Kundu, A., Nigam, K.D.P. and Verma, R.P., Catalyst wetting characteristics in trickle- bed reactors, AIChE journal, vol. 49, no. 9, pp.2253-2263, 2003.

[17] Malgarinos, I., Nikolopoulos, N. and Gavaises, M., Numerical investigation of heavy fuel droplet-particle collisions in the injection zone of a Fluid Catalytic Cracking reactor, Part I: Numerical model and 2D simulations, Fuel Processing Technology, vol. 156, pp.317-330, 2017.

[18] Onishi, V.C., Carrero-Parreño, A., Reyes-Labarta, J.A., Ruiz-Femenia, R., Salcedo-Díaz, R., Fraga, E.S. and Caballero, J.A., Shale gas flowback water desalination: Single vs multiple-effect evaporation with vapor recompression cycle and thermal integration, Desalination, vol. 404, pp.230-248, 2017.

[19] Meiser, I., Müller, S.C., Ehrhart, F., Shirley, S.G. and Zimmermann, H., A new validation method for clinical grade micro-encapsulation: quantitative high speed video analysis of alginate capsule, Microsystem Technologies, vol. 21, no. 1, pp.75-84, 2015.

[20] Moon, B.U., Abbasi, N., Jones, S.G., Hwang, D.K. and Tsai, S.S., Water-in-Water Droplets by Passive Microfluidic Flow Focusing, Analytical chemistry, vol. 88, no. 7, pp.3982-3989, 2016.

[21] Wu, L., Chen, P., Dong, Y., Feng, X. and Liu, B.F., Encapsulation of single cells on a microfluidic device integrating droplet generation with fluorescence-activated droplet sorting, Biomedical microdevices, vol. 15, no. 3, pp.553-560, 2013.

[22] Zagnoni, M. and Cooper, J.M., Droplet microfluidics for high-throughput analysis of cells and particles, Methods Cell Biol, vol. 102, pp.25-48, 2011.

[23] Theberge, A.B., Courtois, F., Schaerli, Y., Fischlechner, M., Abell, C., Hollfelder, F. and Huck, W.T., Microdroplets in microfluidics: an evolving platform for discoveries in chemistry and biology, Angewandte Chemie International Edition, vol. 49, no. 34, pp.5846-5868, 2010.

[24] Yang, C.G., Xu, Z.R. and Wang, J.H., Manipulation of droplets in microfluidic systems, TrAC Trends in Analytical Chemistry, vol. 29, no. 2, pp.141-157, 2010.

[25] Khoufech, A., Benali, M. and Saleh, K., Influence of liquid formulation and impact conditions on the coating of hydrophobic surfaces, Powder Technology, vol. 270, pp.599-611, 2015.

[26] Keshani, S., Daud, W.R.W., Nourouzi, M.M., Namvar, F. and Ghasemi, M., Spray drying: an overview on wall deposition, process and modeling. Journal of Food Engineering, vol 146, pp.152-162, 2015.

[27] Nedovic, V., Kalusevic, A., Manojlovic, V., Levic, S. and Bugarski, B., An overview of encapsulation technologies for food applications, Procedia Food Science, vol. 1, pp.1806-1815, 2011.

[28] Bakry, A.M., Abbas, S., Ali, B., Majeed, H., Abouelwafa, M.Y., Mousa, A. and Liang, L., Microencapsulation of oils: a comprehensive review of benefits, techniques, and applications, Comprehensive Reviews in Food Science and Food Safety, vol. 15, no. 1, pp.143-182, 2016.

[29] Oxley, J. D. Spray cooling and spray chilling for food ingredient and nutraceutical encapsulation. In Encapsulation technologies and delivery systems for food ingredients and nutraceuticals, pp. 110-130. 2012.

[30] Fang, Z. and Bhandari, B. Spray drying, freeze drying and related processes for food ingredient and nutraceutical encapsulation. In Encapsulation technologies and delivery systems for food ingredients and nutraceuticals, pp. 73-109. 2012.

[31] Breitenbach, J. Melt extrusion: from process to drug delivery technology. European Journal of Pharmaceutics and Biopharmaceutics, vol 54, no. 2: 107-117,2002.

[32] A Guide to Injection Moulding., http://www.preview-project.eu/a-guide-to-injection-moulding/blog/.

[33] Kakran, M. and Antipina, M.N., Emulsion-based techniques for encapsulation in biomedicine, food and personal care, Current Opinion in Pharmacology, vol. 18, pp.47-55, 2014.

[34] Dressler, O., Casadevall i Solvas, X. and deMello, A.J., Chemical and Biological Dynamics Using Droplet-Based Microfluidics, Annual Review of Analytical Chemistry, vol. 10, pp. 1-24, 2017

[35] Zuidam, N.J. and Shimoni, E., Overview of microencapsulates for use in food products or processes and methods to make them, In Encapsulation technologies for active food ingredients and food processing (pp. 3-29). Springer, New York, 2010.

[36] Bolleddula, D.A., Berchielli, A. and Aliseda, A., Impact of a heterogeneous liquid droplet on a dry surface: Application to the pharmaceutical industry, Advances in colloid and interface science, vol. 159, no. 2, pp.144-159, 2010.

[37] Bakshi, S., Roisman, I.V. and Tropea, C., Investigations on the impact of a drop onto a small spherical target, Physics of Fluids, vol. 19, no. 3, p.032102, 2007.

[38] Josserand, C. and Thoroddsen, S.T. Drop impact on a solid surface, Annual Review of Fluid Mechanics, vol. 48, pp.365-391, 2016.

[39] Liang, G. and Mudawar, I. Review of mass and momentum interactions during drop impact on a liquid film, International Journal of Heat and Mass Transfer, vol. 101, pp.577-599, 2016.

[40] Marengo, M., Antonini, C., Roisman, I.V. and Tropea, C., Drop collisions with simple and complex surfaces, Current Opinion in Colloid & Interface Science, vol.16, no. 4, pp.292-302, 2011.

[41] Eral, H.B., Manukyan, G. and Oh, J.M., Wetting of a drop on a sphere, Langmuir, vol. 27, no. 9, pp.5340-5346, 2011.

[42] Khojasteh, D., Kazerooni, M., Salarian, S. and Kamali, R., Droplet impact on superhydrophobic surfaces: A review of recent developments, Journal of Industrial and Engineering Chemistry, vol. 42, pp.1-14, 2016.

[43] Khojasteh, D., Mousavi, S.M. and Kamali, R., CFD analysis of Newtonian and non-Newtonian droplets impinging on heated hydrophilic and hydrophobic surfaces, Indian Journal of Physics, vol. 91, no. 5, pp.513-520, 2017.

[44] Mitra, S., Doroodchi, E., Pareek, V., Joshi, J.B. and Evans, G.M., Collision behaviour of a smaller particle into a larger stationary droplet, Advanced Powder Technology, vol. 26, no. 1, pp.280-295, 2015.

[45] Liu, D., He, Q. and Evans, G.M., Penetration behaviour of individual hydrophilic particle at a gas–liquid interface, Advanced Powder Technology, vol. 21, no. 4, pp.401-411, 2010.

[46] Dubrovsky, V.V., Podvysotsky, A.M. and Shraiber, A.A., Particle interaction in three-phase polydisperse flows, International journal of multiphase flow, vol. 18, no. 3, pp.337-352, 1992.

[47] Liang, G., Mu, X., Guo, Y. and Shen, S. Crown and drop rebound on thin curved liquid films, International Journal of Heat and Mass Transfer, vol. 98, pp.455-461, 2016.

[48] Liang, G., Guo, Y., Yang, Y., Guo, S. and Shen, S. Special phenomena from a single liquid drop impact on wetted cylindrical surfaces, Experimental Thermal and Fluid Science, vol. 51, pp.18-27, 2013.

[49] Liang, G., Guo, Y., Mu, X. and Shen, S. Experimental investigation of a drop impacting on wetted spheres, Experimental Thermal and Fluid Science, vol. 55, pp.150-157, 2014.

[50] Rozhkov, A., Prunet-Foch, B. and Vignes-Adler, M., Impact of water drops on small targets, Physics of Fluids, vol. 14, no. 10, pp.3485-3501, 2002.

[51] Yoon, S.S., Kim, H.Y., Lee, D., Kim, N., Jepsen, R.A. and James, S.C., Experimental splash studies of monodisperse sprays impacting variously shaped surfaces, Drying Technology, vol. 27, no. 2, pp.258-266, 2009.

[52] Juarez, G., Gastopoulos, T., Zhang, Y., Siegel, M.L. and Arratia, P.E., Splash control of drop impacts with geometric targets, Physical Review E, vol. 85, no. 2, p.026319, 2012.

[53] Liu, Y., Andrew, M., Li, J., Yeomans, J.M. and Wang, Z., Symmetry breaking in drop bouncing on curved surfaces, Nature communications, vol. 6, 2015.

[54] Sechenyh, V. and Amirfazli, A., An experimental study for impact of a drop onto a particle in mid-air: The influence of particle wettability, Journal of Fluids and Structures, vol. 66, pp.282-292, 2016.

[55] Charalampous, G. and Hardalupas, Y., Collisions of droplets on spherical particles, Physics of Fluids, vol. 29, no. 10, p.103305, 2017.

[56] Banitabaei, S.A. and Amirfazli, A., Droplet impact onto a solid sphere: Effect of wettability and impact velocity, Physics of Fluids, vol. 29, no. 6, p.062111, 2017.

[57] Mitra, S., Evans, G.M., Doroodchi, E., Pareek, V. and Joshi, J.B., Interactions in droplet and particle system of near unity size ratio, Chemical Engineering Science, vol. 170, pp. 154-175, 2017.

[58] Chen, S. and Bertola, V., Drop impact on spherical soft surfaces, Physics of Fluids, vol. 29, no. 8, p.082106, 2017.

[59] Jadidbonab, H., Mitroglou, N., Karathanassis, I. and Gavaises, M., Experimental study of Diesel fuel droplet impact onto similar size polished spherical heated solid particle, Langmuir, vol. 34, no. 1, pp.36-49, 2017.

[60] Pasandideh-Fard, M., Bussmann, M. and Chandra, S., Simulating droplet impact on a substrate of arbitrary shape, Atomization and sprays, vol. 11, no. 4, 2001.

[61] Yan- Peng, L. and Huan- Ran, W., Three- dimensional direct simulation of a droplet impacting onto a solid sphere with low- impact energy, The Canadian Journal of Chemical Engineering, vol. 89, no. 1, pp.83-91, 2011.

[62] Gac, J.M. and Gradoń, L., Lattice-Boltzmann modeling of collisions between droplets and particles, Colloids and Surfaces A: Physicochemical and Engineering Aspects, vol. 441, pp.831-836, 2014.

[63] Zhang, D., Papadikis, K. and Gu, S., Investigations on the droplet impact onto a spherical surface with a high-density ratio multi-relaxation time lattice-Boltzmann model, Communications in Computational Physics, vol. 16, no. 4, pp.892-912, 2014.

[64] Gumulya, M., Utikar, R.P., Pareek, V., Mead-Hunter, R., Mitra, S. and Evans, G.M., Evaporation of a droplet on a heated spherical particle, Chemical Engineering Journal, vol. 278, pp.309-319, 2015.

[65] Malgarinos, I., Nikolopoulos, N. and Gavaises, M., A numerical study on droplet-particle collision dynamics, International Journal of Heat and Fluid Flow, vol. 61, pp.499-509, 2016.

[66] Liu, X., Zhao, Y., Chen, S., Shen, S. and Zhao, X., Numerical research on the dynamic characteristics of a droplet impacting a hydrophobic tube, Physics of Fluids, vol. 29, no. 6, p.062105, 2017.

[67] Bordbar, A., Taassob, A., Khojasteh, D., Marengo, M., and Kamali, R., Maximum Spreading and Rebound of a Droplet Impacting onto a Spherical Surface at low Weber numbers, Langmuir, vol. 34, no. 17, p.5149-5158, 2018

[68] Levin, Z. and Hobbs, P.V., Splashing of water drops on solid and wetted surfaces: hydrodynamics and charge separation, Philosophical Transactions of the Royal Society of London A: Mathematical, Physical and Engineering Sciences, vol. 269, pp.555-585, 1971.

[69] Hardalupas, Y., Taylor, A.M.K.P. and Wilkins, J.H., Experimental investigation of sub-millimetre droplet impingement on to spherical surfaces, International journal of heat and fluid flow, vol. 20, no. 5, pp.477-485, 1999.

[70] Zhu, Y., Liu, H.R., Mu, K., Gao, P., Ding, H. and Lu, X.Y., Dynamics of drop impact onto a solid sphere: spreading and retraction, Journal of Fluid Mechanics, vol. 824, 2017.

[71] Guo, C., Sun, J., Sun, Y., Wang, M. and Zhao, D. Droplet impact on cross-scale cylindrical superhydrophobic surfaces, Applied Physics Letters, vol. 112, no. 26, p.263702, 2018.

[72] Akao, F., Deformation behaviors of a liquid droplet impinging onto hot metal surface, Trans. Int. Steel Inst. Japan, vol. 20, pp.737-743, 1980.

[73] Scheller, B.L. and Bousfield, D.W., Newtonian drop impact with a solid surface, AIChE Journal, vol. 41, no. 6, pp.1357-1367, 1995.

[74] Clanet, C., Béguin, C., Richard, D. and Quéré, D., Maximal deformation of an impacting drop, Journal of Fluid Mechanics, vol. 517, pp.199-208, 2004.

[75] Roisman, I.V., Inertia dominated drop collisions. II. An analytical solution of the Navier–Stokes equations for a spreading viscous film, Physics of Fluids, vol. 21, no. 5, p.052104, 2009.

[76] Liang, G. and Mudawar, I. Review of drop impact on heated walls, International Journal of Heat and Mass Transfer, vol. 106, pp.103-126, 2017.

[77] Liang, G. and Mudawar, I. Review of spray cooling–Part 1: single-phase and nucleate boiling regimes, and critical heat flux, International Journal of Heat and Mass Transfer, vol. 115, pp.1174-1205, 2017.

[78] Mitra, S., Nguyen, T.B.T., Doroodchi, E., Pareek, V., Joshi, J.B. and Evans, G.M., On wetting characteristics of droplet on a spherical particle in film boiling regime, Chemical Engineering Science, vol. 149, pp.181-203, 2016.
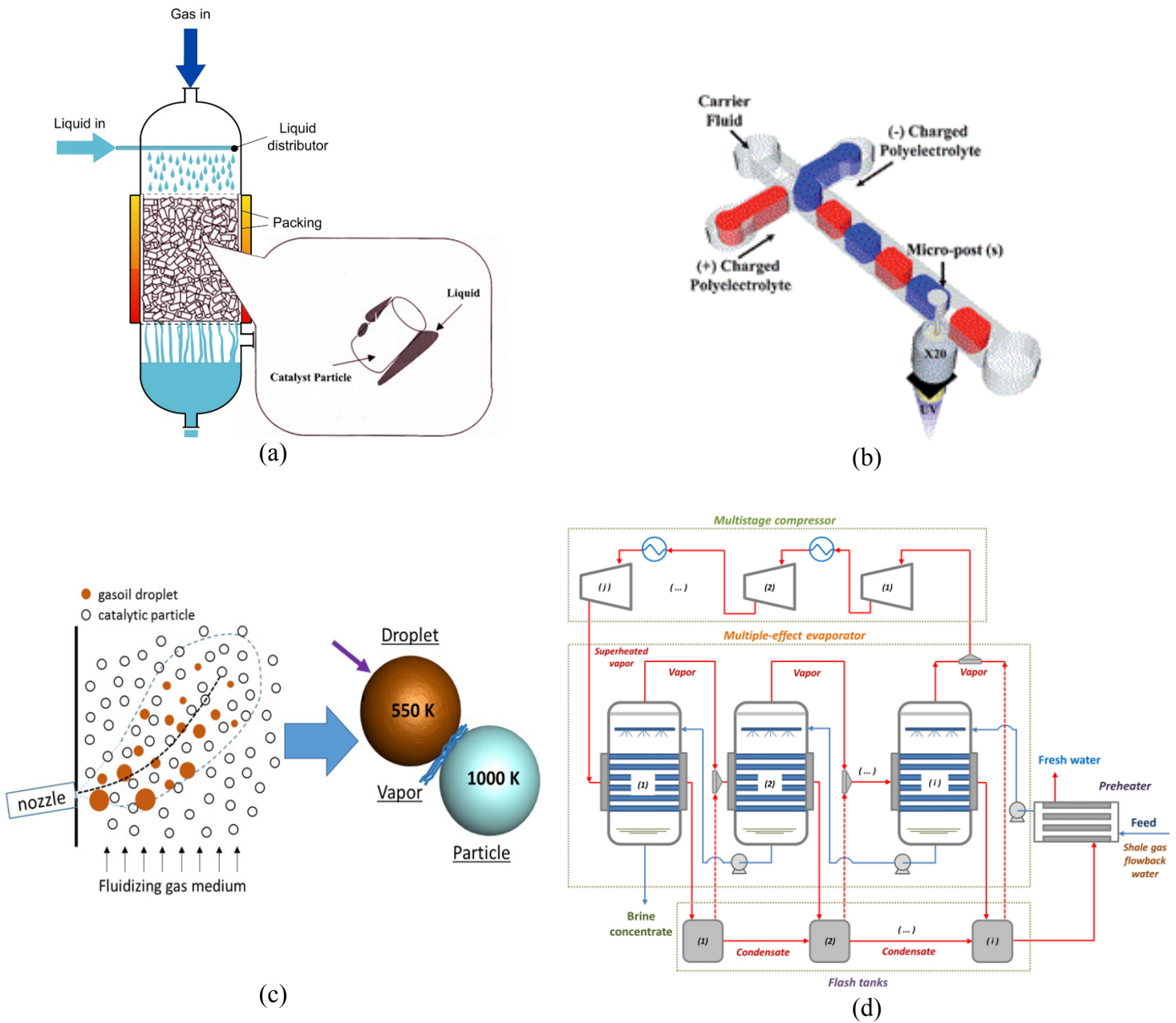
Fig. 1: Different applications of droplet impact on spherical surfaces: a) a trickled bed reactor [16]; b) layer-by-layer (LbL) deposition in a microfluidic device [12]; c) a fluidized catalytic cracking (FCC) process [17]; d) multi-effect desalination process [18].
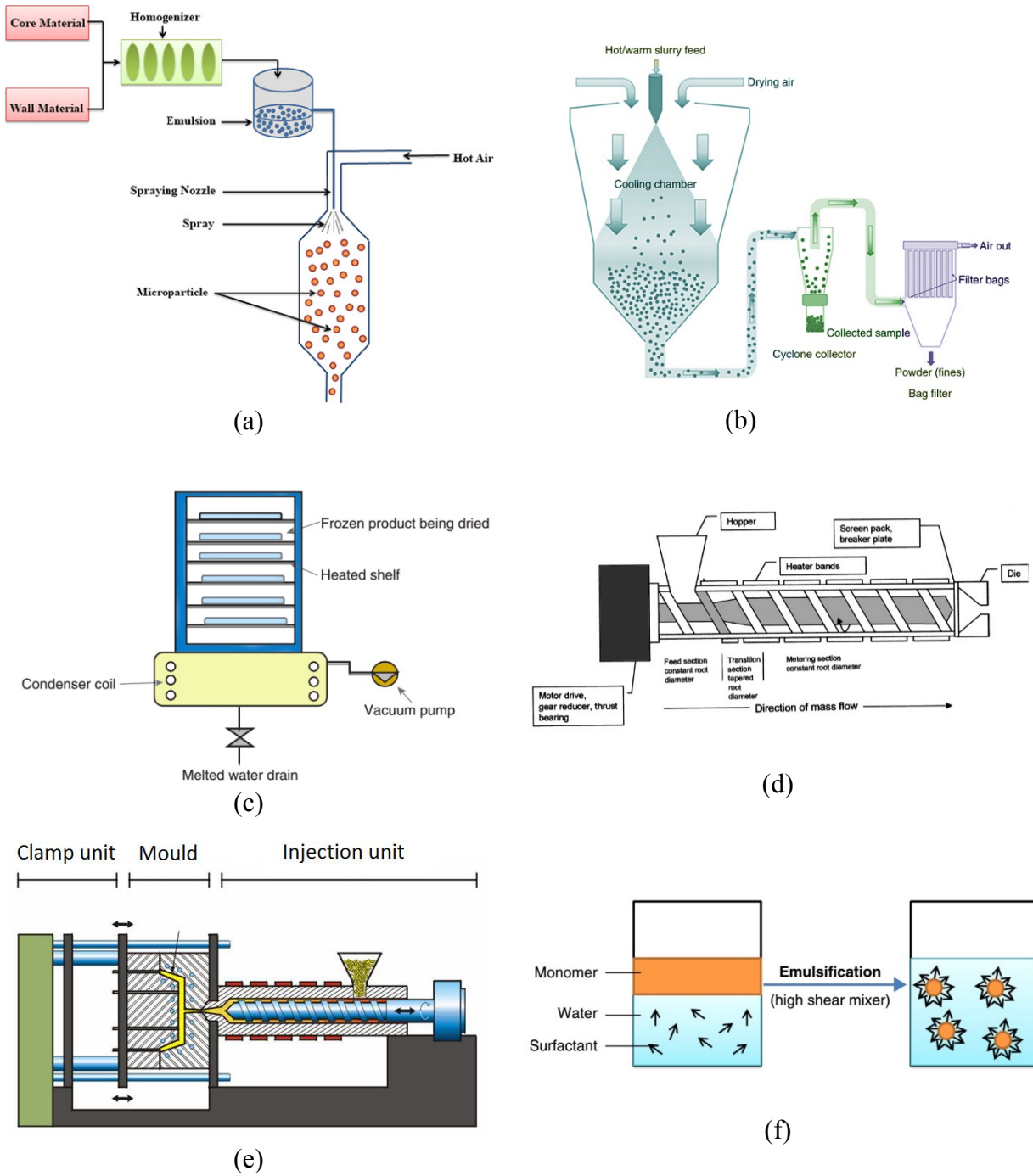
Fig. 2: Microencapsulation process by a) spray-drying [28]; b) spray-chilling [29]; c) freeze-drying [30]; d) melt-extrusion [31]; e) melt-injection [32]; f) emulsification [33].
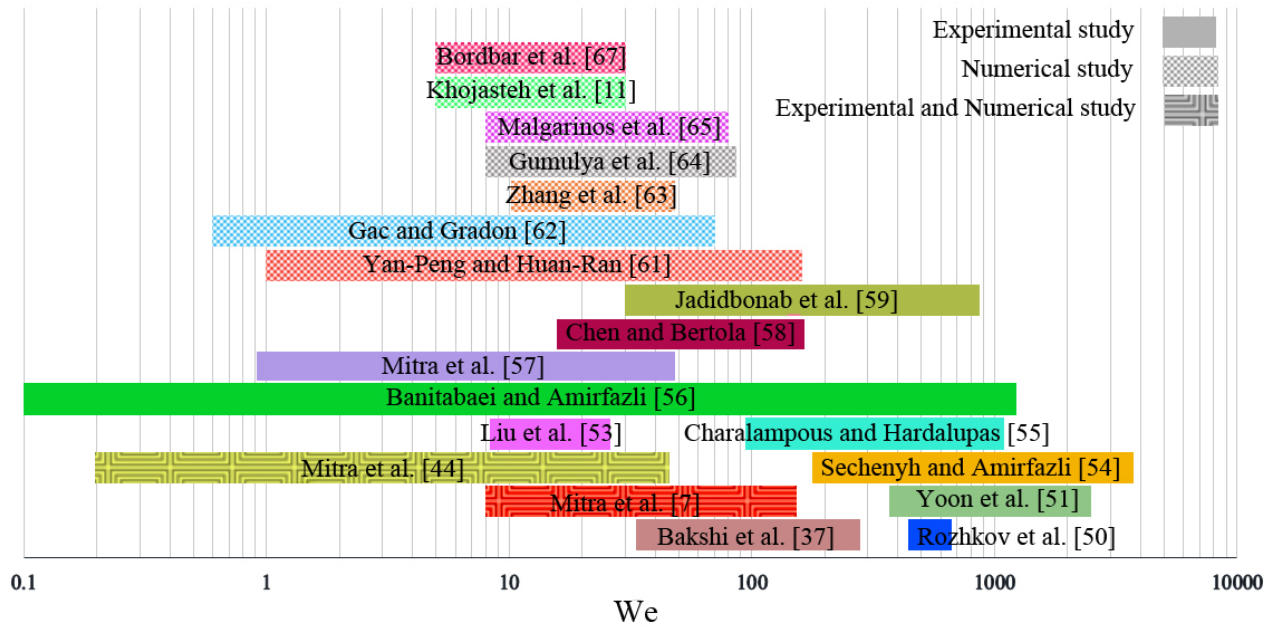
Fig. 3: Weber ranges for the existing literature on droplet impact onto spherical particles.
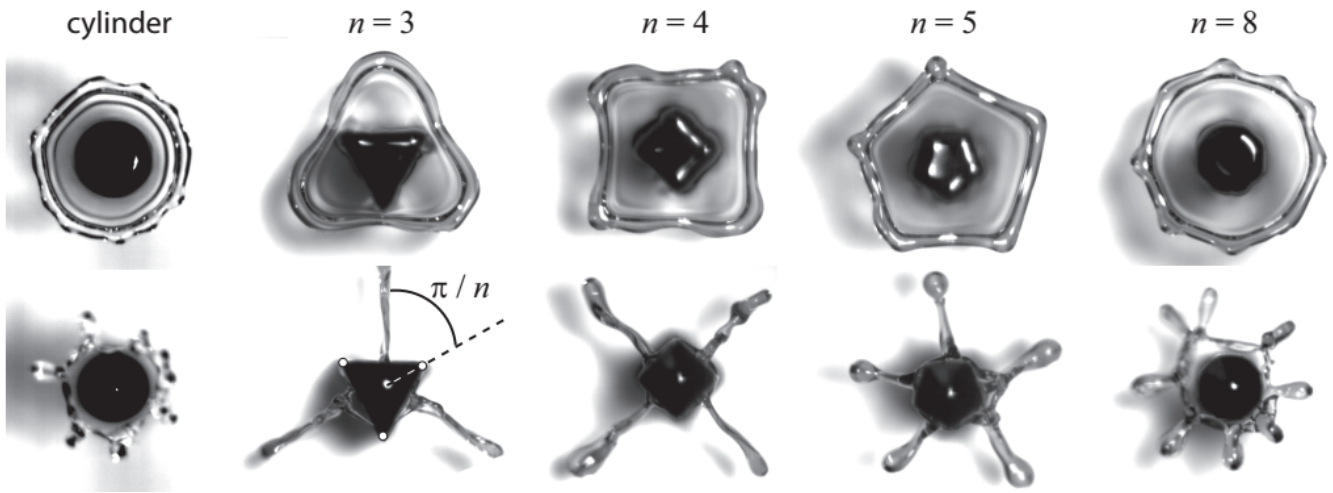
Fig. 4: Top view of drop impact on geometric target posts. Geometrically-shaped lamella after impact with a cylindrical, triangular (n = 3), square (n = 4), pentagon (n = 5), and octagon (n = 8) post (Top row). Filament formation after impact shows that the splashing dynamics depend on the target cross-sectional geometry (Bottom row) [52].
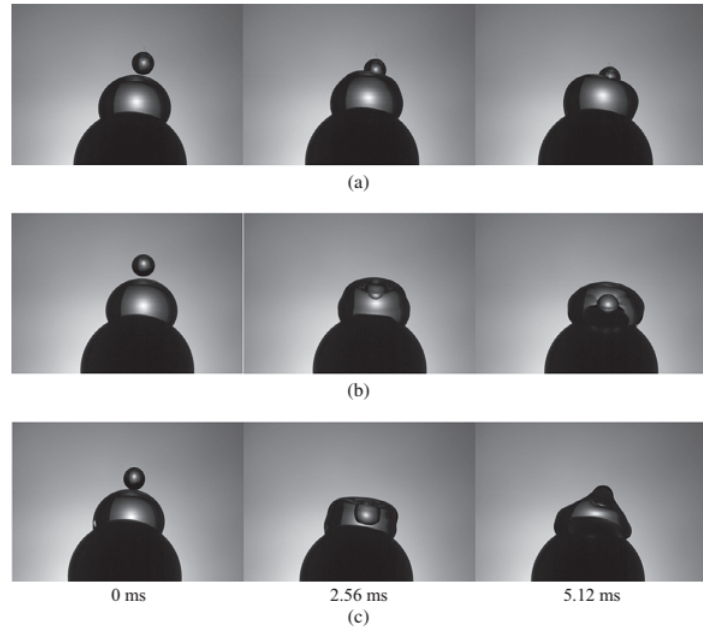
Fig. 5: Time-lapsed images of particle collision dynamics on the droplet at different *We* numbers: (a) *We* = 0.9 (partial submerge of particle); (b) *We* = 5.3 (sinking of particle to the bottom of the droplet); (c) *We* = 12.4 (reaching of particle to the bottom of the droplet) [44].
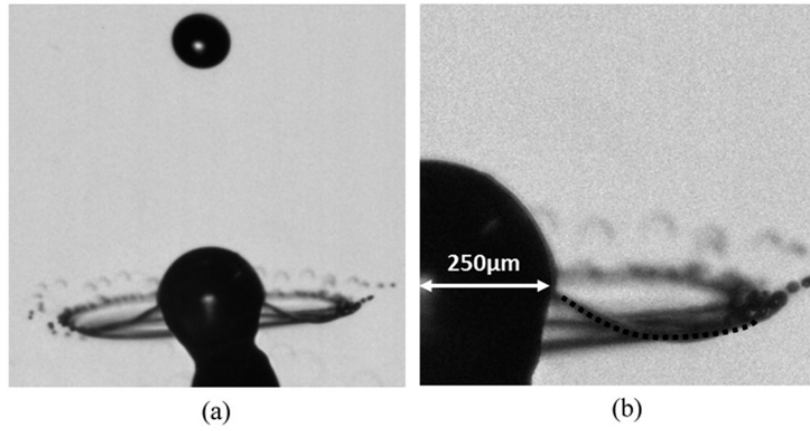
Fig. 6: (a) Liquid film ejecting from the particle surface; (b) detailed view of (a) where the satellite

droplets formed can be seen. The dotted line highlights the curvature of the crown [55].
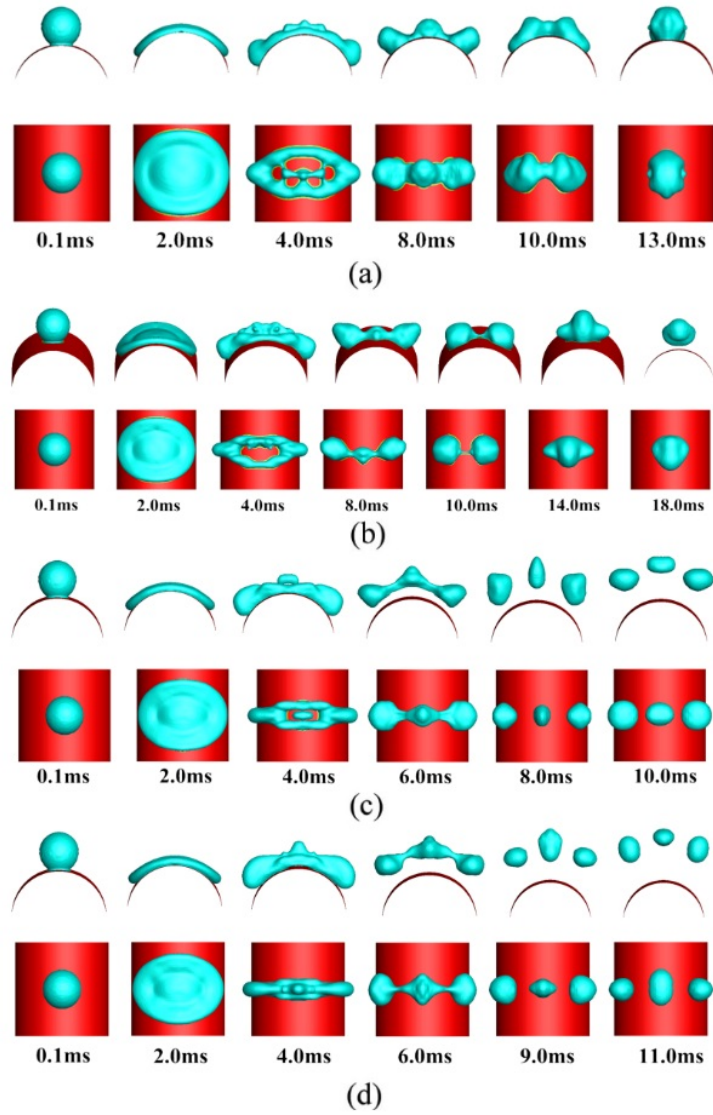
Fig. 7: The regime of droplet impact on the tubular surface with a CA of (a) 107°, (b) 120°, (c) 135° and (d) 153° [66].
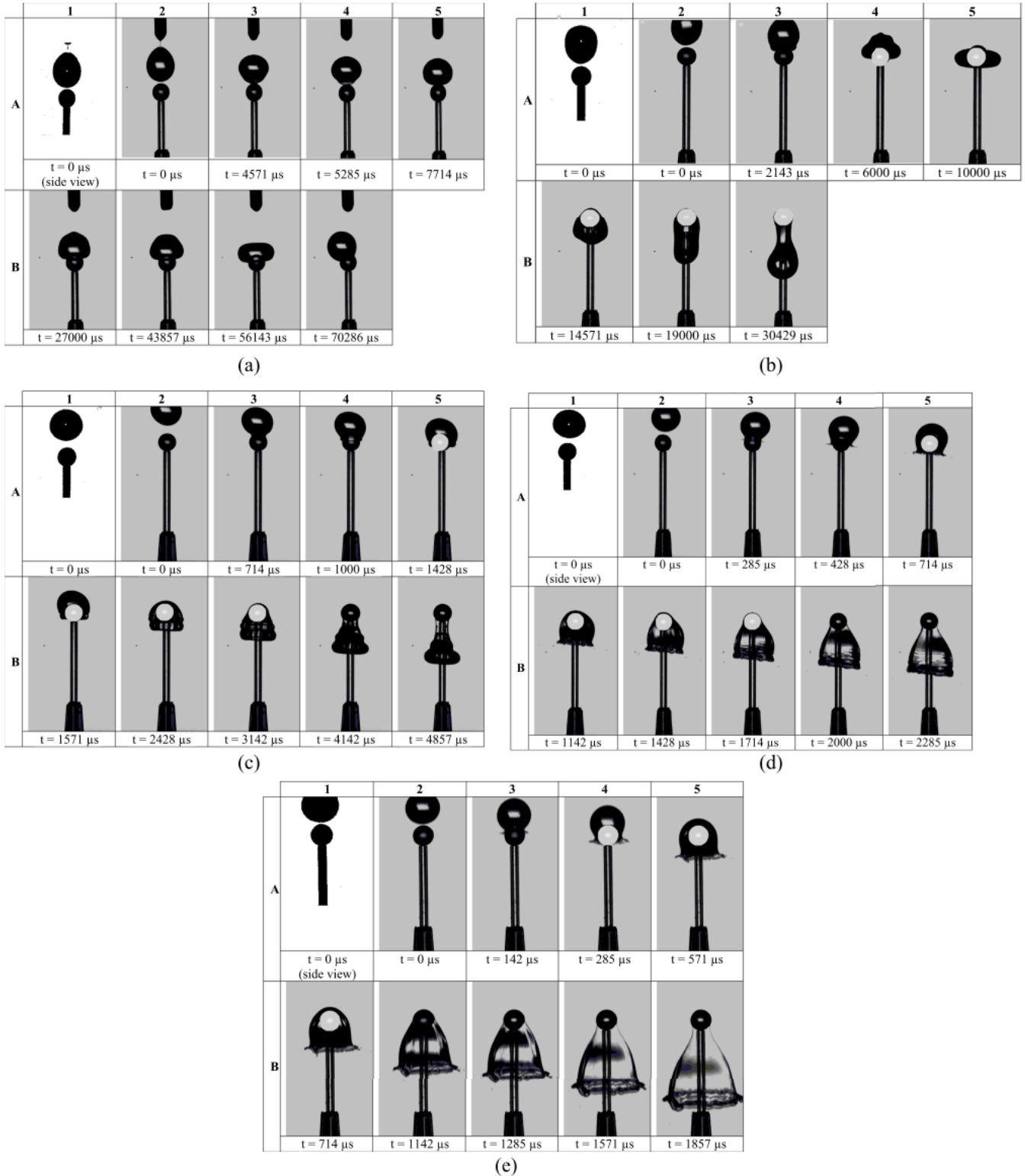
Fig. 8: The temporal deformations of droplet after impacting an H particle (D* = 0.57, CA = 118º) for different impact velocities of: (a) 0.05 m/s, (b) 0.4 m/s, (c) 1.8 m/s, (d) 3.26 m/s, (e) 5.00 m/s [56].
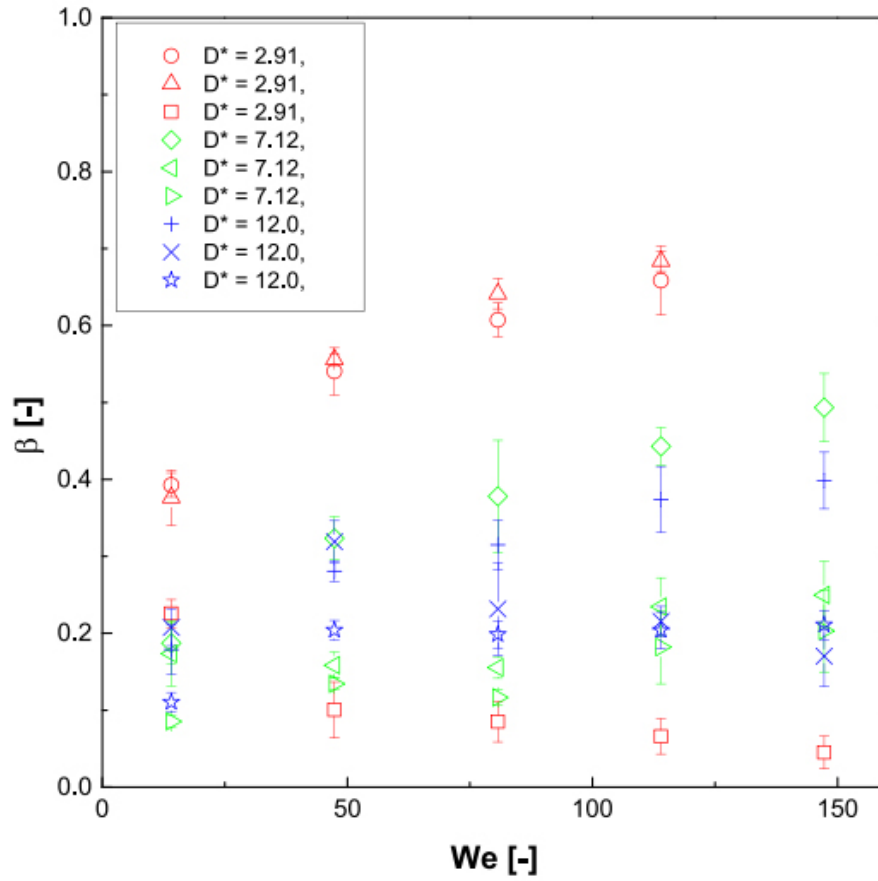
Fig. 9: Retraction coefficient as a function of impact *We* number for different particle to drop diameter

ratios [58].
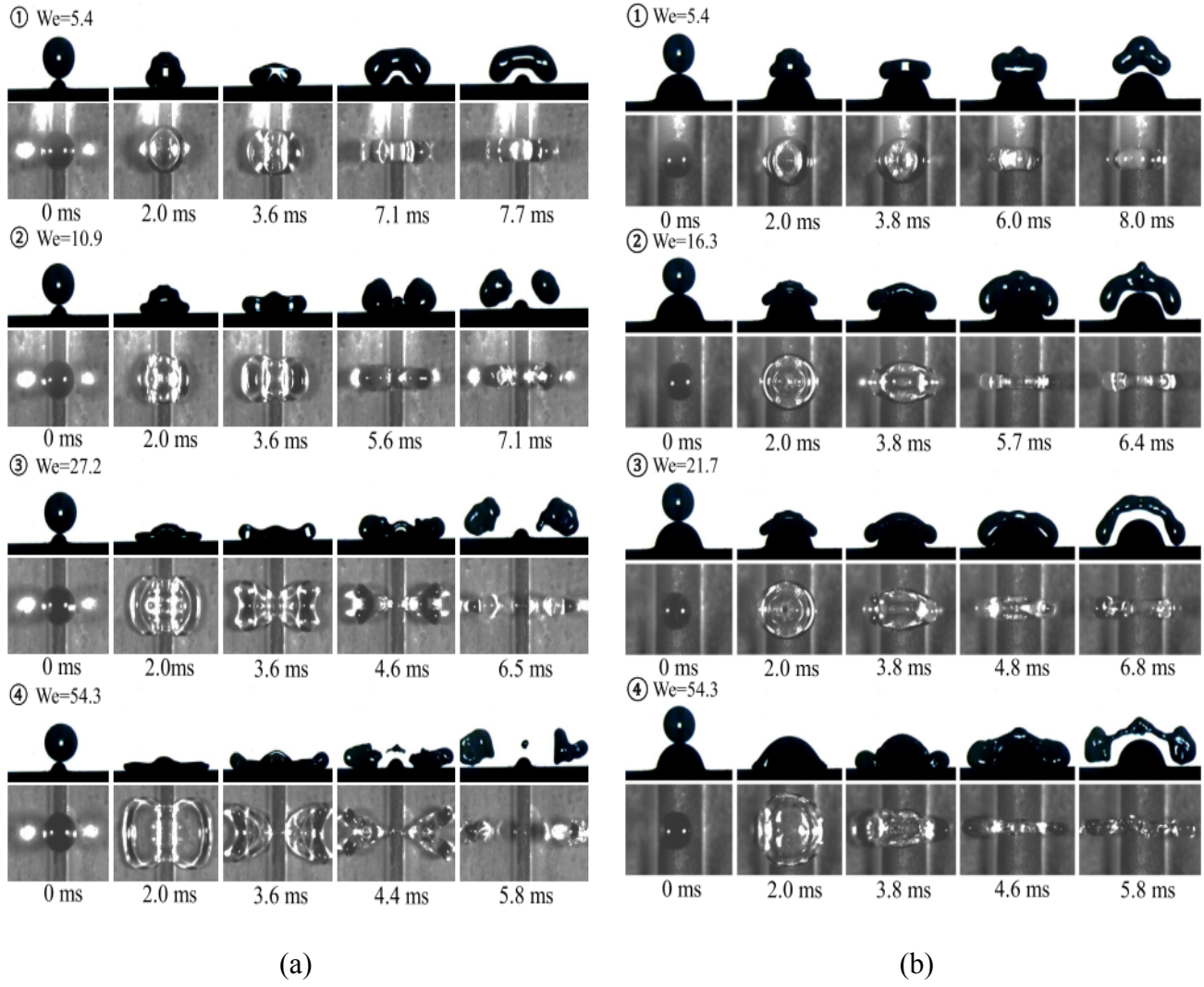
Fig. 10: Snapshots of droplets impacting on the cylindrical surfaces for: (a) D* = 0.5, (b) D* = 1.5 [71].
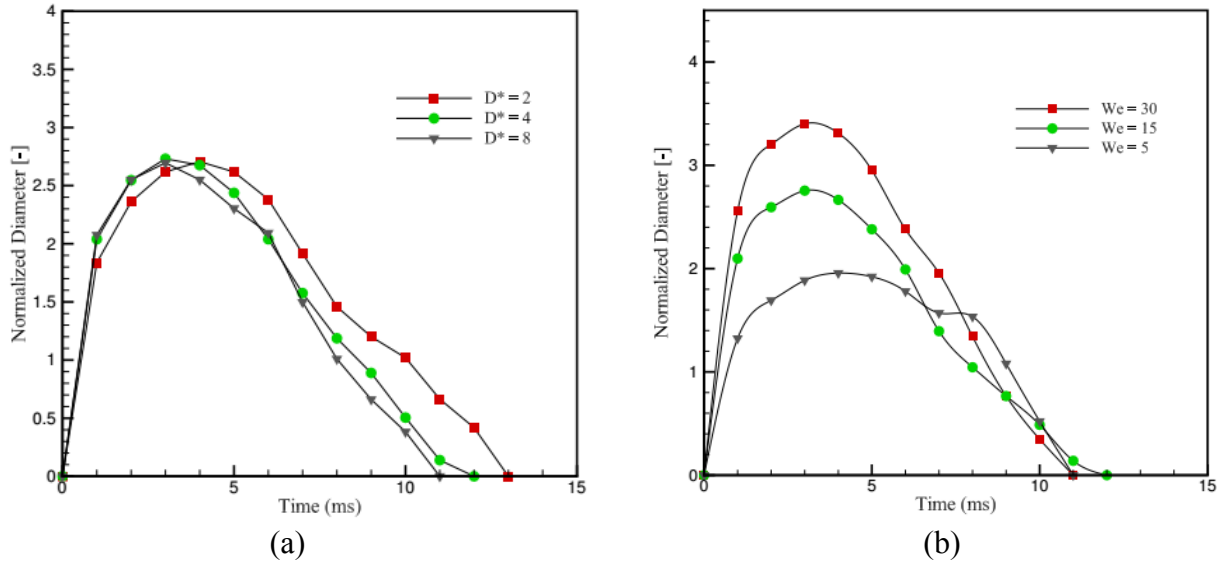
Fig. 11: Normalized diameter of the droplet impacting a SH sphere with CA of 163º: (a) effect of curvature when $We = 15$; (b) effects of varying We numbers [67].

| $t = 3\ ms$ | $t = 6\ ms$ | $t = 9\ ms$ | $t = 12\ ms$ | $t = 15\ ms$ |
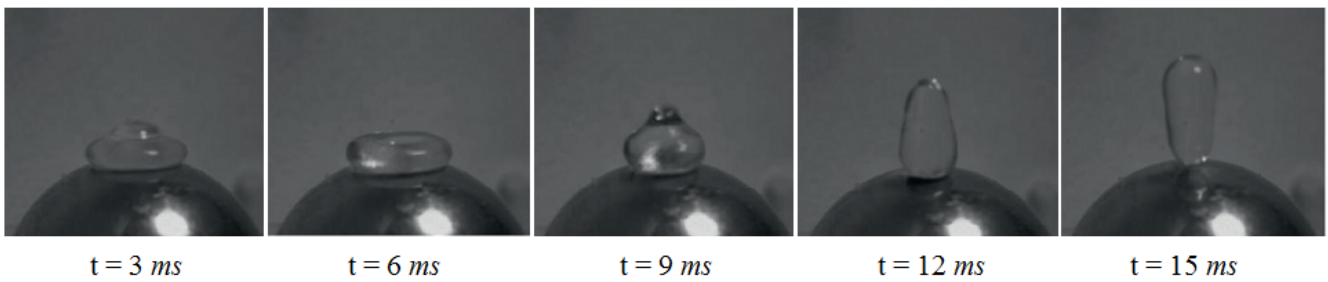
Fig. 12: Time evolution of a water droplet impinging a spherical target with the surface temperature of 250 ºC at $We = 8$ [7].
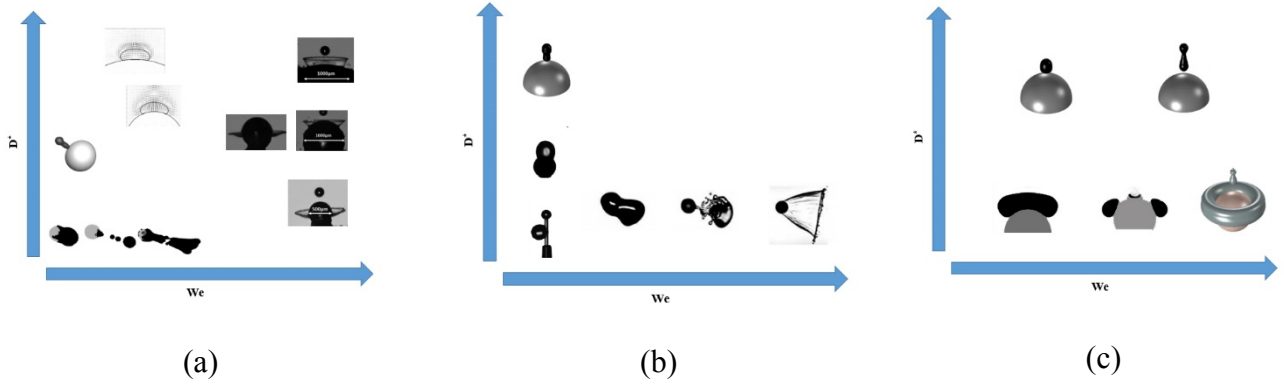
Fig. 13: A summary of droplet-particle collision outcomes for: a) HP surfaces; b) H surfaces; c) SH surfaces.

Table 1: List of experimental investigations and their most important findings regarding droplet impacting onto solid spherical surfaces.

Authors	Droplet dimension or size ratio	Dimensionless numbers	Type of surface	Main outcomes
Rozhkov et al. [50]	Water (2.8–4.0 mm diameter)	$448 < We < 664$ $9486 < Re < 13746$	HP (CA: ND) Stainless steel disk (3.9 mm diameter)	For collision of water drops against small targets: • liquid ejection in the shape of a central cap is produced • this cap is surrounded by a liquid lamella
Bakshi et al. [37]	Water/ Glycerine-water solution/ Isopropanol $1.23 < D* < 8.80$	$35 < We < 287$ $780 < Re < 5525$	HP (CA: ND) Stainless steel	The dynamics of film thickness variation on the spheres comprise three distinct phases: • initial deformation phase • inertia dominated phase • viscosity dominated phase
Yoon et al. [51]	Water/ Diesel (250 μm diameter)	$375 < We < 2370$	HP (CA: ND) Aluminium rod (2mm diameter)	For drop impact on the convex tip of a rod: • diameter of the splashed corona is diminished • horizontal momentum is decreased
Mitra et al. [7]	Water (3.1mm diameter)/ Isopropyl alcohol (2.1mm diameter)/ Acetone (2.1mm diameter)	$8 < We < 136$	HP Brass particle (10 mm diameter)	• Heat transfer coefficients during impact is reduced towards film boiling regime
Juarez et al. [52]	Water and glycerol solution (2.85 mm diameter)	$We = 250$ $Re = 550$	HP (CA: ND) Polyoxymethylene (sectional geometry: cylinder and regular polygon shapes)	• Drop splashing is controlled by geometric features of the target.
Mitra et al. [44]	Water $D* = 0.33, 1.75$	$0.2 < We < 13.5$ $120 < Re < 1036$	HP and H (CAs: 55° and 90°)	With decrease in sinking time: • transition from partial to complete penetration is observed

			Glass ballotini and polypropylene	• significant shape deformation of the droplet occurs
Liu et al. [53]	Water D* = 2.8	7.9 < *We* < 23.6	SH (CA: 160°) Echevaria leaf (curvature diameter between 4 and 20 mm)	For a drop impacting Echevaria leaves: • asymmetric bouncing dynamics is observable • distinct spreading and retraction happen along two perpendicular directions
Sechenyh and Amirfazli [54]	Water (2.9 mm diameter)	181 < *We* < 2526 Target: 2mm bead	HP and H (CAs: ND) Polystyrene/ soda-lime glass beads of 2mm)	• Quantitative aspects for dynamics of the lamella and liquid ligaments for mid-air collisions are provided. • Wettability of the particle plays a dominant role in collision outcomes with formation of a liquid lamella and ligaments
Charalampous and Hardalupas [55]	Water 1.81 < D* < 11.11	92 < *We* < 1015 0.0070 < *Oh* < 0.0089	HP (59° < CA < 67°) Glass	• A new outcome (besides splashing and deposition), unique to droplet-particle collisions is introduced
Banitabaei and Amirfazli [56]	Water D* = 0.57	0.1 < *We* < 1146	HP and H (CAs: 70°, 90°,118°) Glass bead (2mm diameter)	• For H targets, lamella geometry is not affected by the extent of hydrophobicity • A thin liquid film is formed for high velocity impact of droplet onto a H particle
Mitra et al. [57]	Water and glycerol solution 1.16 < D* < 1.2	0.9 < *We* < 47.1 400 < *Re* < 2878	H (CA=86°)	• A novel technique for non-invasive laser heating of particle is developed to investigate non-isothermal interactions
Chen and Bertola [58]	Water 2.91 < D* < 12	14 < *We* < 147	H, polydimethylsiloxane (PDMS)	• Droplet experiences a more pronounced withdrawal phenomenon by an increase in curvature of the surface
Jadidbonab et al. [59]	Diesel D* = 2.5	30 < *We* < 850 210 < *Re* < 1135	HP Brass	The maximum spreading factor of a diesel droplet: • increases with an increase in impact *We* number • rises with a decrease in particle temperature

Table 2: List of numerical investigations and their most important findings regarding droplet impacting onto solid spherical surfaces.

Authors	Method	Dimensionless numbers	Droplet dimension or size ratio	Type of surface	Main outcomes
Pasandideh-Fard et al. [60]	Finite-difference solution of the Navier-Stokes equations.	ND	Water droplet with 2mm diameter.	HP, Stainless steel tubes with diameters between 0.5 to 6.35mm.	• The smaller the radius of the cylinder at which the drop impacts, the less liquid is attached to the solid surface
Yan-Peng and Huan-Ran [61]	Level-set method coupled with the interfacial cell immersed boundary method	$1 < We < 150$ $Oh = 0.0831$	$2 < D* < 10$	HP (CA=87°), Surface material: ND	• A local breakage phenomenon is occurred in the centre of the droplet when hitting a smaller sphere during its first recoiling stage
Gac and Gradon [62]	Two-colour lattice-Boltzmann model	$0.6 < We < 70$ $0.8 < Ca < 7$	$0.63 < D* < 1.3$	HP (CA: ND) Surface material: ND	Three scenarios of a collision between droplets and particles are recognized: • Coalescence • Ripping and coating • Skirt scattering
Zhang et al. [63]	Two-dimensional multi-relaxation time (MRT) lattice Boltzmann model	$10.4 < We < 46.27$ $28.27 < Re < 217.5$	ND	H and HP, Surface material: ND $60° < CA < 107°$	• Surface tension dominates the retraction phase. • Transition to the retraction phase occurs earlier for low We numbers
Gumulya et al. [64]	Combined LS/VOF	$8 < We < 84$ $1300 < Re < 4370$	Water $D* = 4.2$	H Target material: Brass	• Maximum spread of droplet and heat transfer rate depend mainly on We number • Rate of droplet recoil depends on Re number

Malgarinos et al. [65]	VOF coupled with local refinement technique	$8 < We < 80$	Water $0.8 < D^* < 3.22$	HP (CA: 90°)	Inertial forces dominate over the viscous, gravitational and surface tension forces at the early stages of impact
Liu et al. [66]	Coupled Level-Set/VOF	ND	Water (1.72 mm diameter)	H and SH (107° < CA <153°) Target material: Aluminium tube (4mm diameter)	Characteristics of spread, splash, and rebound are related to: • pressure field inside and outside the liquid film • velocity field inside and outside the liquid film
Khojasteh et al. [11]	Level-Set Method	$5 < We < 30$	Water $D^* = 2$ and 4	H and SH (CAs =125° and 163°)	Impact on spherical surfaces generally provides: • a higher area of liquid to be in contact with the substrate than the case of flat surfaces
Bordbar et al. [67]	Level-Set Method	$5 < We < 30$	Water $1 < D^* < 8$	H and SH (CAs =125° and 163°)	• A new practical model is provided • This model is able to predict the maximum spreading of low We numbers impact of droplets onto H and SH spherical solid surfaces

Table 3. Modified models to predict the spreading factor of drop impact on spherical particles [11].

Model	Spreading factor (D_{max}/D_0) – flat surfaces	Spreading factor (D_{max}/D_0) – curved surfaces
Akao et al. [72]	$0.613We^{0.39}$	$We^{0.39}$
Scheller and Bousfield [73]	$0.61Re^{1/5}(WeRe^{-2/5})^{1/6}$	$0.95Re^{1/5}(WeRe^{-2/5})^{1/6}$
Clanet et al. [74]	$We^{1/4}$	$1.5We^{1/4}$
Roisman [75]	$0.87Re^{1/5} - 0.4Re^{2/5}We^{-1/2}$	$1.5Re^{1/5} - 0.6Re^{2/5}We^{-1/2}$